

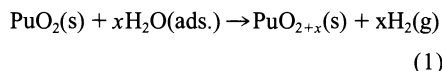
Reaction of Plutonium Dioxide with Water: Formation and Properties of PuO_{2+x}

John M. Haschke,^{1*} Thomas H. Allen,² Luis A. Morales²

Results show that PuO_{2+x} , a high-composition ($x \leq 0.27$) phase containing Pu(VI), is the stable binary oxide in air. This nonstoichiometric oxide forms by reaction of dioxide with water and by water-catalyzed reaction of dioxide with oxygen. The $\text{PuO}_2 + \text{H}_2\text{O}$ reaction rate is 0.27 nanomoles per meter squared per hour at 25°C; the activation energy at 25° to 350°C is 39 kilojoules per mole. Slow kinetics and a low lattice parameter–composition dependence for fluorite-related PuO_{2+x} are consistent with a failure to observe the phase in earlier studies. Perplexing aspects of plutonium oxide chemistry can now be explained.

A fundamental tenet of plutonium chemistry has been that PuO_2 is the highest composition binary oxide (1–3). That description is based on estimated thermodynamic properties suggesting that higher oxides are unstable (4) and on unsuccessful attempts by early workers to prepare higher oxides in experiments with strong oxidants such as atomic oxygen, ozone, and nitrogen dioxide (5, 6). Higher oxides were also not seen during thermal decomposition of Pu(VI) carbonates (7). Excess mass gains observed during atmospheric oxidation of plutonium metal were attributed to adsorption of water on the high-surface area product (2, 8). However, results of a recent x-ray diffraction (XRD) and x-ray photoelectron spectroscopy (XPS) study of the adherent oxide formed on Pu metal by reaction in water vapor at 250°C showed that a higher oxide formed at the gas-oxide interface had a fluorite-related structure and contained Pu(VI) (9).

Here we show that PuO_{2+x} , the stable oxide in air, is formed by reaction of PuO_2 with adsorbed water in at 25° to 350°C.



Mass spectrometric analyses show that H_2 is the only gaseous product. Oxidation rates (R) measured at constant temperature and H_2O pressure by microbalance (MB) and pressure-volume-temperature (PVT) methods (10–12) were constant over a range of oxide composition as shown by representative linear pressure-time (P - t) data (Fig. 1) and by mass-time curves. Pressure-time data for 25°C gave an R of 0.13 $\text{nmol O m}^{-2} \text{ hour}^{-1}$. The initial oxide composition ($\text{PuO}_{1.97}$) used in these tests was as determined from XRD results

and lattice parameter (a_o)–composition data for $\text{PuO}_{2.8}$ (13). The x value was 0.17 after the test at 350°C and changed by 0.003 in 4 years at 25°C, but the maximum oxide composition was not attained at any temperature.

The rate of Eq. 1 at 25°C is also derived from P - t and mass spectrometric data obtained after exposing PuO_2 to a 2:1 molar mixture of H_2 and O_2 . Water formed in situ by surface-catalyzed association of the elements (14) was not detected by mass spectrometry, but remained chemisorbed as OH^- on the oxide surface (15) and caused a progressive decrease in the $\text{H}_2 + \text{O}_2$ combination rate as active sites were blocked. After more than 100 days, the OH^- concentration reached 15 to 20% of monolayer coverage on the oxide and the P - t curve became linear as O_2 reacted at a constant rate (0.25 $\text{nmol O m}^{-2} \text{ hour}^{-1}$) characteristic of the $\text{PuO}_2 + \text{H}_2\text{O}$ reaction.

Data for H_2 generation by reaction of high-surface area (750 $\text{m}^2 \text{ g}^{-1}$) PuO_2 during hydrolysis of Pu in aqueous salt solution (16, 17) give a rate of 0.42 $\text{nmol O m}^{-2} \text{ hour}^{-1}$ for Eq. 1. Three independent results give an average R of $0.27 \pm 0.17 \text{ nmol O m}^{-2} \text{ hour}^{-1}$ at 25°C and show that the reaction rate is independent of adsorbed H_2O over a concentration range extending from fractional surface coverage by OH^- to saturation in liquid water. Oxidation is sufficiently slow that the oxidation rate at 25°C is maintained by chemisorbed H_2O at less than 20% monolayer coverage by OH^- .

Results show that the rate of the $\text{PuO}_2 + \text{H}_2\text{O}$ reaction is a function of temperature as described by an Arrhenius relation (Fig. 2) with an activation energy of $39 \pm 3 \text{ kJ/mol}$. This result is consistent with chemical reaction and suggests that the contribution from temperature-independent radiolysis of water by decay of plutonium isotopes was negligible in our experiments.

Diffraction and spectroscopic data are consistent with a solid solution PuO_{2+x} phase

formed by accommodating a high oxidation state of plutonium and interstitial oxygen in the fluorite structure of PuO_2 . Earlier XPS analysis of the oxide formed during oxidation of metal by water (9) showed peaks with high binding energies (442 and 429 eV for the $4f_{5/2}$ and $4f_{7/2}$ spectra, respectively) correlated with either the Pu(VI) or Pu(VII) oxidation state and indicating the absence of Pu(V). The O 1s spectrum is consistent with the presence of oxygen as oxide. We attribute the absence of OH^- to continuing reaction after placement in the spectrometer. XRD data for oxides that we synthesized showed fluorite-related face-centered cubic structures and a surprisingly low composition dependence of a_o (Fig. 3). The lattice parameter reached a minimum (5.3975 Å) at $\text{PuO}_{2.00}$, increased sharply over a narrow composition range, and increased linearly with O:Pu to values in excess of $\text{PuO}_{2.25}$.

Insensitivity of a_o to PuO_{2+x} composition is consistent with substitution of Pu(VI) for Pu(IV) on cationic sites of a fluorite structure and accommodation of additional O^{2-} in octahedral interstices. This structural model is supported by analogy to UO_{2+x} (18) and by neutron diffraction results (19). Substitution of Pu(VI) tends to shrink the lattice, but addition of O^{2-} causes expansion. These opposing changes are apparently of comparable magnitude and result in a low O:Pu dependence of a_o . The sharp increase in a_o at compositions immediately above that of dioxide suggests that onset of PuO_{2+x} formation is accompanied by expansion of the entire lattice. Frequent appearance of short induction periods at the beginning of rate measurements may result from sluggish lattice dynamics.

Results for the oxide prepared by hydrolysis of Pu in salt solution at room temperature (16, 17) confirm the a_o -composition dependence (Fig. 3) and demonstrate that PuO_{2+x} is unstable at elevated temperatures in the absence of water or oxygen. H_2 formed dur-

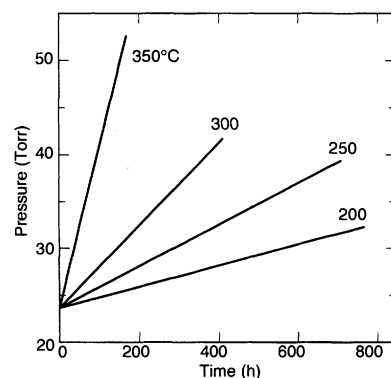


Fig. 1. Time dependence of the H_2 pressure during exposure of PuO_2 to H_2O vapor at experimental temperatures and a constant water pressure of 32 mbar (24 torr).

¹11003 Willow Bend Drive, Waco, TX 76712, USA.
²Los Alamos National Laboratory, Los Alamos, NM 87545, USA.

*To whom correspondence should be addressed. E-mail: haschketoo@aol.com

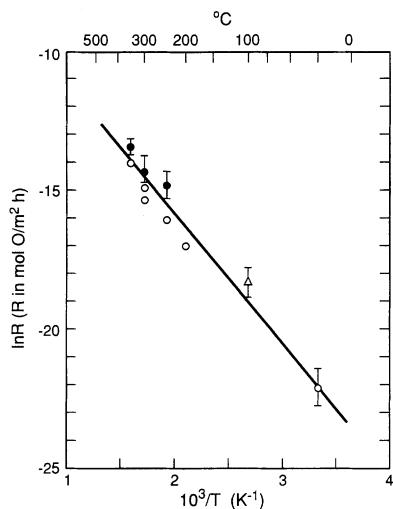


Fig. 2. Arrhenius analysis of rate-temperature data for the $\text{PuO}_2 + \text{H}_2\text{O}$ reaction at 25° to 350°C and 32-mbar H_2O pressure. Data from MB and PVT measurements are indicated by filled and open circles, respectively. The data point at 100°C (triangle) was determined by using the extent of reaction derived from a_o of the product and the lattice parameter-composition correlation (Fig. 3). The Arrhenius equation is $\ln R = -6.441 - (4706/T)$.

ing the $\text{Pu} + \text{H}_2\text{O}$ reaction and continued to form as progressive oxidation produced plutonium monoxide monohydride (PuOH) and a series of oxide hydride and oxide phases. H_2 production continued beyond the dioxide composition in a process that we can now explain by Eq. 1. The measured a_o (5.404 \AA) of the $\text{PuO}_{2.265}$ product obtained when the test was arbitrarily terminated agrees closely with the correlation derived for O:Pu ratios in the 2.016 to 2.169 range. Thermogravimetric analysis at 25° to 500°C and a_o for the fired oxide showed that PuO_{2+x} decomposes to PuO_2 upon heating in a vacuum (17).

Our results show that PuO_{2+x} is formed in moist air or moist oxygen via a catalytic cycle (Fig. 4) driven by Eq. 1. We observed that water formed and accumulated on the oxide surface as H_2 and O_2 dissociatively adsorbed and associated as H_2O , while oxygen simultaneously disappeared at a constant rate characteristic of the $\text{PuO}_2 + \text{H}_2\text{O}$ reaction. As shown by the cycle, adsorbed H_2O reacts to form PuO_{2+x} . However, in the presence of O_2 , atomic H that formed on the oxide by the $\text{PuO}_2 + \text{H}_2\text{O}$ reaction does not associate as H_2 , but reacts with dissociatively adsorbed oxygen to re-form H_2O . The net result of the cyclic process is the reaction of PuO_2 and O_2 at the rate of $\text{PuO}_2 + \text{H}_2\text{O}$. Water enhances the rate of PuO_{2+x} formation, while the oxide surface catalyzes re-formation of water. This catalytic cycle accounts for all observations in this study, as well as for transformation of isotopically labeled O_2^* into H_2O^* during oxidation of uranium (20).

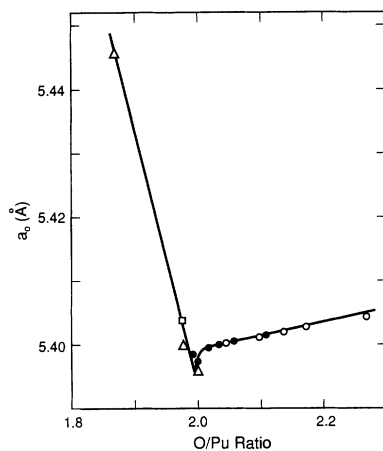


Fig. 3. Dependence of the cubic lattice parameter (a_o) on oxide composition (O:Pu ratio = $2 \pm x$) of the PuO_{2-x} and PuO_{2+x} phases at room temperature. Reference lattice parameter-O:Pu data for $\text{PuO}_{2.6}$ from Gardner *et al.* (13) are shown by triangles and a_o of the starting oxide ($\text{PuO}_{1.97}$) is shown by a square. Values of a_o obtained for products from MB and PVT measurements are shown by filled and open circles, respectively. The lattice parameter-composition dependence of PuO_{2+x} is given by $a_o (\text{Å}) = 5.3643 + 0.01746 \text{ O:Pu}$.

The descriptive chemistry of plutonium is confused by conflicting reports that the dioxide is green (1) or dull yellow to khaki (3). We observed that the dioxide is yellow to buff, but that PuO_{2+x} consistently has an intense green color.

Our results show that PuO_{2+x} is the thermodynamically stable oxide of plutonium in air at temperatures below 350°C and contradict earlier evidence that higher oxides are unstable and cannot be prepared. Failure to observe PuO_{2+x} may have resulted from several factors. The stability range was probably exceeded by reaction temperatures ($1000^\circ \pm 100^\circ\text{C}$) of some studies (21). Exposure of the dioxide to strong oxidants increases the free energy for reaction, but does not necessarily enhance the kinetics. Although oxidation by O_2 is thermodynamically more favorable than oxidation by H_2O , reaction of dry oxygen is slow and the extent is limited after a few-hour experiment (6). If oxidation occurred, its detection by XRD is unlikely because of the low a_o -O:Pu dependence of PuO_{2+x} (Fig. 3) and the expectation that a_o would decrease with increasing x as for UO_{2+x} (21). Oxidation by water is also slow, but readily detected by production of H_2 , a sensitive and definitive indicator of PuO_{2+x} formation.

PuO_{2+x} apparently participates in moisture-enhanced corrosion of the metal (9, 14). Reaction of adsorbed water with PuO_2 contributes to H_2 pressurization of sealed storage containers (22) until the equilibrium pressure of Eq. 1 is reached. As with uranium oxide, the presence of hexavalent cations should increase oxide solubility. Elimination of Pu(VI) by decomposi-

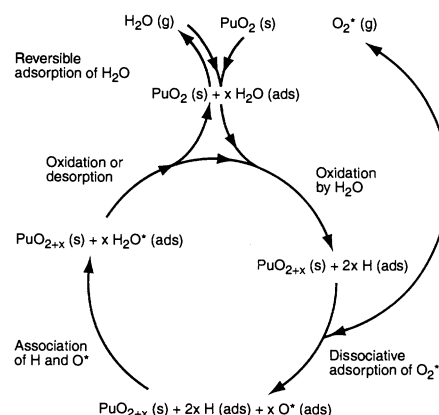


Fig. 4. The chemical cycle for H_2O -catalyzed $\text{PuO}_2 + \text{O}_2$ reaction and oxide-catalyzed regeneration of H_2O .

tion of PuO_{2+x} during calcination may account for slow dissolution of "high fired" oxide in aqueous acids (1, 3). Leaching of accumulated Pu(VI) from PuO_{2+x} formed by water-catalyzed oxidation of PuO_2 in air accounts for the appearance of Pu(VI) as the predominant species in water coexisting with oxide (23) and may be important in the surprisingly rapid (1.3 km in 30 years) groundwater migration of plutonium (24).

References and Notes

1. J. M. Cleveland, *The Chemistry of Plutonium* (American Nuclear Society, La Grange Park, IL, 1979), pp. 291-322.
2. J. T. Waber, in *Plutonium Handbook*, O. J. Wick, Ed. (American Nuclear Society, La Grange Park, IL, 1980), pp. 145-189.
3. F. Weigel, J. J. Katz, G. T. Seaborg, in *The Chemistry of the Actinide Elements*, J. J. Katz, G. T. Seaborg, L. R. Morss, Eds. (Chapman & Hall, New York, 1986), vol. 1, pp. 680-702.
4. L. Brewer, *Chem. Rev.* **52**, 1 (1953).
5. E. F. Westrum, in *The Transuranium Elements*, G. T. Seaborg, J. J. Katz, W. M. Manning, Eds. (National Nuclear Energy Series IV, 14B, paper 6.57, McGraw-Hill, New York, 1949), pp. 936-944.
6. J. J. Katz and D. M. Gruen, *J. Am. Chem. Soc.* **71**, 2106 (1949).
7. R. Marquart, G. Hoffmann, F. Weigel, *J. Less Common Met.* **91**, 119 (1983).
8. J. F. Sackman, in *Plutonium 1960*, E. Grisson, W. B. H. Lord, R. D. Fowler, Eds. (Cleaver-Hume, London, 1961), pp. 222-229.
9. J. L. Stakebake, D. T. Larson, J. M. Haschke, *J. Alloys Compd.* **202**, 251 (1993).
10. J. M. Haschke and T. H. Allen, *Rep. LA-13537-MS* (Los Alamos National Laboratory, Los Alamos, NM, 1999).
11. L. A. Morales, J. M. Haschke, T. H. Allen, *Rep. LA-13597-MS* (Los Alamos National Laboratory, Los Alamos, NM, 1999).
12. Oxides prepared by oxidizing electrorefined weapons-grade Pu (100 part per million Am) in air ($\text{PuO}_{1.97}$) or the gallium alloy in O_2 ($\text{PuO}_{2.00}$) had specific surface areas of 11.3 and $4.0 \pm 3 \text{ m}^2 \text{ g}^{-1}$, respectively, and were contained in Pt or stainless steel during exposure to H_2O vapor for periods up to 4 years. Constant H_2O pressures ($25 \pm 7 \text{ mbar}$) were maintained by using isothermal water reservoirs. Temperatures were measured in the gas phase near the oxides. Oxidation rates in units of $\text{mol O m}^{-2} \text{ hour}^{-1}$ were defined by slopes of mass/P-t data; x was defined by terminal MB and PVT data and Eq. 1. Details are reported elsewhere (10, 11), and interpretation is augmented by results of an experiment in which $\text{PuO}_{2.00}$ was exposed to a 2:1 molar mixture of D_2 and O_2 at 170 mbar (10).

13. E. R. Gardner, T. L. Markin, R. S. Street, *J. Inorg. Nucl. Chem.* **27**, 541 (1965).
14. J. M. Haschke, T. H. Allen, J. L. Stakebake, *J. Alloys Compd.* **243**, 23 (1996).
15. J. M. Haschke and T. E. Ricketts, *J. Alloys Compd.* **252**, 148 (1997).
16. J. M. Haschke, A. E. Hodges, G. E. Bixby, R. L. Lucas, *Rep. RFP-3476* (Rocky Flats Plant, Golden, CO, 1983).
17. J. M. Haschke, in *Transuranium Elements: A Half Century*, L. R. Morss and J. Fuger, Eds. (American Chemical Society, Washington, DC, 1992), pp. 416–425.
18. C. A. Colmenares, *Prog. Solid State Chem.* **9**, 139 (1975).
19. L. A. Morales and A. C. Lawson, unpublished data.
20. M. McD. Baker, L. N. Ness, S. Orman, *Trans. Faraday Soc.* **62**, 2525 (1966).
21. C. E. Holley *et al.*, Proceedings of the Second United Nations International Conference on the Peaceful Uses of Atomic Energy, Geneva, Switzerland, 1–13 September 1958 (United Nations, Geneva, 1958), vol. 6, pp. 215–220.
22. J. M. Haschke and J. C. Martz, in *Encyclopedia of Environmental Analysis and Remediation*, R. A. Meyers, Ed. (Wiley, New York, 1998), vol. 6, pp. 3740–3755.
23. R. C. Dahlman, E. A. Bondietti, L. D. Eyeman, in *Actinides in the Environment*, A. M. Friedman, Ed. (American Chemical Society Symposium. Series No. 35, Washington, DC, 1976), pp. 47–80.
24. A. B. Kersting *et al.*, *Nature* **397**, 56 (1999).
25. This work was performed under U.S. Department of Energy Contract W-7405-ENG-36.

28 September 1999; accepted 18 November 1999

Communication Through a Diffusive Medium: Coherence and Capacity

Aris L. Moustakas,^{1*} Harold U. Baranger,^{1,2} Leon Balents,^{1,3}
Anirvan M. Sengupta,¹ Steven H. Simon¹

Coherent wave propagation in disordered media gives rise to many fascinating phenomena as diverse as universal conductance fluctuations in mesoscopic metals and speckle patterns in light scattering. Here, the theory of electromagnetic wave propagation in diffusive media is combined with information theory to show how interference affects the information transmission rate between antenna arrays. Nontrivial dependencies of the information capacity on the nature of the antenna arrays are found, such as the dimensionality of the arrays and their direction with respect to the local scattering medium. This approach provides a physical picture for understanding the importance of scattering in the transfer of information through wireless communications.

The ongoing communications revolution has motivated researchers to look for novel ways to transmit information (1, 2). One recent development (3, 4) is the suggestion that, contrary to long-held beliefs, random scattering of microwave or radio signals may enhance the amount of information that can be transmitted on a particular channel. Prompted by this suggestion, we introduce a realistic physical model for a scattering environment and analytically evaluate the amount of information that can be transmitted between two antenna arrays for a number of example cases. On the one hand, this lays a new foundation for complex microwave signal modeling, an important task in a world with ever-increasing demand for wireless communication, and on the other, it introduces a new arena for physicists to test ideas concerning disordered media.

From information theory (5), the capacity of a channel between a transmitter and a receiver, that is, the maximum rate of information transfer at a given frequency, can be described in terms of the average power

of the signal S and the noise N at the receiver: $C = \log_2(1 + S/N)$. More generally (2), the communication channel connecting several transmitters and receivers is described by a matrix $G_{i\alpha}$ giving the amplitude of the received signal α due to transmitter i . The information carried by the channel can be characterized by using several quantities, such as the capacity or mutual information, which are typically functionals of the matrix G , which must be known in order to predict these quantities. Often G cannot be predicted for actual systems, such as wireless communication networks or optical fibers, because of the complicated scattering and interference of waves that are involved. It is crucial, therefore, to develop physical models for the signal propagation, because it is only through such models that one can understand the real effects of scattering and interference on the amount of information that can be communicated.

In many cases, only partial information is available for prediction; in these situations, one has only a statistical description of G . Instead of making assumptions about G directly, which is the usual procedure in information theory, we introduce statistical models for the physical environment from which we derive the properties of G . The advantage of this procedure is that simple physical models can yield very nontrivial properties of G .

Statistical descriptions of the environment have been quite successful in the physics of disordered media (6–9). The simplest of these is diffusive propagation. In our case of electromagnetic propagation in the context of wireless communication, diffusion is known to work well in various circumstances (10), and simple extensions seem relevant for many others. From a diffusive approach, one finds the moments of the distribution of G . These will enable us to calculate information-theoretic quantities (for example, the capacity) using a replica field theory approach to random matrix theory (11). Implicit in this approach is the assumption that the full distribution of G is sampled, which is realistic in many real-world situations where the environment is changing. However, when the number of antennas is large, many quantities of interest become strongly peaked around their average and this assumption can be relaxed.

In a statistical description, the scattering of the signal is characterized by the mean-free path, ℓ , corresponding roughly to the distance between scattering events. When ℓ is large compared to the wavelength λ but small compared to the distance d between the two arrays, the wave propagation becomes diffusive (8, 9). This has been analyzed previously in the context of electron diffusion in metals (6, 7) and light propagation in solids (8, 12). In the case of wireless propagation, with signals in the 2-GHz region, $\lambda \sim 10$ to 15 cm, while ℓ is on the order of meters for indoors and tens of meters for outdoors propagation, so diffusion is applicable.

In the diffusive regime $\lambda \ll \ell$, to leading order in λ/ℓ , only the quadratic correlations $\langle G_{i\alpha} G_{j\beta}^* \rangle$ are nonnegligible and therefore describe the system, where the brackets represent an average over realizations of the disorder. Higher cumulants of G are of higher order in λ/ℓ . Therefore, the distribution of G is Gaussian with zero average (6–9). The leading term in $\langle G_{i\alpha} G_{j\beta}^* \rangle$ is evaluated by a summation of so-called ladder diagrams (8) corresponding to processes in $\langle G_{i\alpha} G_{j\beta}^* \rangle$ where the waves from antennas i to α and from j to β propagate through the scattering medium along identical paths except for segments of order ℓ at each end.

In several realistic situations discussed be-

¹Bell Labs, Lucent Technologies, 700 Mountain Avenue, Murray Hill, NJ 07974, USA. ²Department of Physics, Duke University, Durham, NC 27708–0305, USA. ³Department of Physics, University of California, Santa Barbara, CA 93106, USA.

*To whom correspondence should be addressed. E-mail: arislm@physics.bell-labs.com